PHYSICAL REVIEW B

CONDENSED MATTER

THIRD SERIES, VOLUME 44, NUMBER 8 15 AUGUST 1991-II

Far-infrared conductivity of TaS_3: The intrinsic charge-density-wave excitation modes

W. N. Creager, P. L. Richards, and A. Zettl

Department of Physics, University of California at Berkeley, Berkeley, California 94720
and Materials Sciences Division of the Lawrence Berkeley Laboratory, Berkeley, California 94720

(Received 28 March 1991)

The far-infrared (FIR) reflectance of the charge-density-wave (CDW) conductor TaS_3 has been measured from 3 to 700 cm^{-1}, over the temperature range from 15 to 300 K. For incident radiation polarized parallel to the long axis of the crystals, a strong reflection edge correlated with the formation of the CDW appears near 80 cm^{-1}. The associated conductivity shows the pinned acoustic phason near 0.5 cm^{-1} dominating $\epsilon(\omega)$ and an additional small mode near 9 cm^{-1}. The size of the latter mode is in sharp contrast to that observed in the related CDW materials $(TaSe_4)_2I$ and $K_{0.3}MoO_3$. These results rule out current models of a "generic FIR mode" in CDW excitations.

A recent far-infrared (FIR) study demonstrated that, in addition to the established charge-density-wave (CDW) excitation modes (dielectric relaxation, the pinned acoustic phason, and single-particle Peierls-gap excitations[1]) the CDW conductor $(TaSe_4)_2I$ has a giant conductivity mode in the FIR frequency range between the acoustic phason and the Peierls gap.[2] Reinterpretation of several previously published conductivity data sets on the blue bronze $K_{0.3}MoO_3$ shows that this CDW conductor most probably also has a distinct giant FIR mode.[2] Hence, a very prominent fourth IR-active mode exists in the two CDW materials for which the full ac response spectrum is known.[3]

It has been suggested that the giant FIR mode observed in $(TaSe_4)_2I$ and $K_{0.3}MoO_3$ may be generic to all CDW conductors and, on this basis, several general CDW conductivity models have been constructed. On the other hand, both $(TaSe_4)_2I$ and $K_{0.3}MoO_3$ are relatively complicated CDW systems (as discussed below), and it is possible that the giant FIR mode arises from peculiarities of these materials.

We report on FIR reflectivity measurements of the CDW conductor TaS_3 which, together with previous microwave[4,5] and optical[6,7] measurements, complete the excitation spectrum for this system. From the FIR reflectance in the CDW state, we show conclusively that in TaS_3, no FIR mode exists comparable in size to the giant mode seen in two other CDW materials. The strengths and frequencies of smaller FIR modes are determined. From these results, we rule out all current models predicting a generic giant FIR mode and place constraints on any new models. The applicability of a zone-folding model is evaluated.

High-purity crystals of TaS_3 were grown by conventional vapor transport methods. In order to prepare a sample suitable for FIR reflectance studies, several thousand single crystals were aligned by hand into an opaque mat 1 cm in diameter. The crystals in the mat were held in place by a trace amount of a plastic resin.[8] An independent check of the resin alone showed it to have no strong modes in the FIR frequency range and no spectral features in common with those measured for the crystal mat. The sample temperature could be varied from 15 to 300 K using a continuous-flow He refrigerator. Polarized light from a Michelson Fourier-transform spectrometer illuminated the sample, and the reflected light was detected by a composite bolometer[9] operated at 1.5 K. Reflection measurements were made at numerous temperatures both above and below the CDW transition temperature $T_p = 220$ K, with light polarized parallel and perpendicular to the chain axis. The reflectance for perpendicular polarization is nearly temperature independent except for the emergence of phonon features. We shall here discuss measurements with light polarized parallel to the chain (long) axis of the crystal.

Figure 1 shows the measured FIR reflectance of TaS_3 at room temperature (dashed line) and at 15 K, in the CDW state well below T_p (solid line). Neglecting the low-frequency Fabry-Pérot oscillations due to the measurement apparatus,[10] a substantial drop in the 15-K reflectance begins at about 40 cm^{-1}, culminating in a sharp fall from about 75% at 60 cm^{-1} to about 6% at 76 cm^{-1}. This dramatic reflection edge near 70 cm^{-1} begins to develop at about 200 K, just below T_p, and it sharpens continuously as the temperature is lowered. Beyond the reflectance edge, there is a series of narrow peaks in the

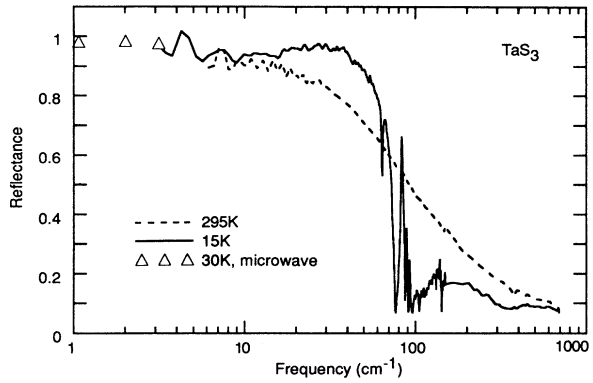

FIG. 1. Reflectance vs frequency for TaS_3 at 15 and 295 K. The triangles are reflectances calculated from microwave frequency conductivities measured at 30 K in Ref. 4.

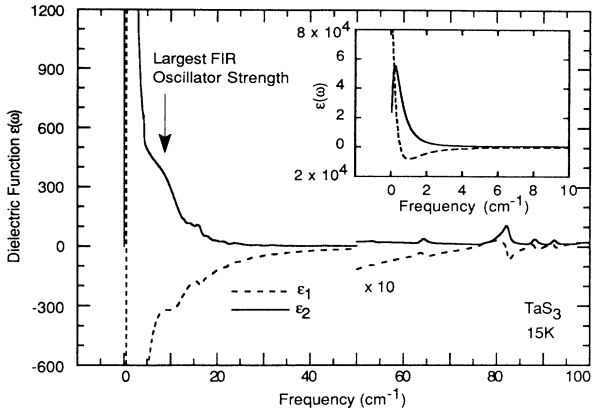

FIG. 2. Reϵ (dashed line) and Imϵ (solid line) deduced by a Kramers-Kronig analysis of the 15-K reflectivity data for TaS_3. Above 50 cm^{-1}, the vertical scales are expanded by a factor of 10.

reflectance at 83, 89, and 92 cm^{-1} followed by a broad maximum centered at 150 cm^{-1}. The low-temperature reflectance stabilizes to about 9% at 300 cm^{-1} and remains featureless and flat out to 700 cm^{-1}. We note the absence of any outstanding feature near 500 cm^{-1} that might be associated with the 500-cm^{-1} anomaly[7] observed in transverse-polarized bolometric absorption spectra of TaS_3.

The complex dielectric function $\epsilon(\omega)$ is most directly obtained from the reflectance via a Kramers-Kronig calculation, for which it is desirable to have reflectance data over as wide a frequency range as possible. For this purpose we have generated effective reflectance data for frequencies below our experimental limit of 3 cm^{-1} by converting microwave conductivity data previously measured[4] on TaS_3 to reflectance. These microwave data points are shown as triangles in Fig. 1; they agree well with the trend of our measured reflectance at low frequencies. The Fabry-Pérot oscillations in our data between 3 and 11 cm^{-1} have been smoothed.[10] The Peierls gap[6] is expected to affect the reflectance near 1200 cm^{-1}. Modeling of this gap was found to have little effect on the dielectric function calculated at lower frequencies, so the high-frequency reflectance was simply continued at its 700-cm^{-1} value.

Figure 2 shows the complex dielectric function $\epsilon(\omega)$ for TaS_3 calculated from the smoothed and extended 15-K reflectance. The vertical scale has been expanded above 50 cm^{-1} to show detailed structure at high frequencies. The inset shows the low-frequency behavior of $\epsilon(\omega)$ more clearly. Figure 2 shows that ϵ_1 crosses from its large positive value at zero frequency to negative values at about 0.5 cm^{-1}, reflecting the pinned acoustic phason mode near this frequency. At higher frequencies, ϵ_1 then recovers and slowly climbs to another zero crossing that corresponds to the dramatic infrared reflectance edge we observe between 70 and 80 cm^{-1}.

Aside from the dominant phason mode observed below 1 cm^{-1} in Fig. 2, there are several other identifiable modes that modify the gradual rise in ϵ_1 and affect the location of the zero crossing. To determine the relative strengths of these smaller modes, we fit them to independent oscillators. The strongest mode lies near 8.9 cm^{-1} and is marked by an arrow in Fig. 2. By considering the uncertainties in the measurement and the smoothing we establish an upper limit $\Omega_p^2 \leq 6.8\times10^{26}$ on its oscillator strength, a factor of 40 or more smaller than that of the giant FIR mode[2] in $(TaSe_4)_2I$ at 38 cm^{-1}. All the modes at frequencies greater than 60 cm^{-1} have oscillator strengths $\Omega_p^2 \leq 9.0\times10^{25}$.

Our FIR measurements of TaS_3 essentially complete the excitation spectrum for this material. In Fig. 3, a comparison is made between the real part of the ac conductivity $\sigma(\omega)$ of TaS_3 and that of $(TaSe_4)_2I$ over a wide frequency range. The TaS_3 data in Fig. 3(a) near the Peierls gap are an approximate conversion from the bolometric absorption spectrum published previously by another group.[6] The line below 2×10^{13} Hz is the FIR conductivity determined from our study. It was calculated as described above using a low-frequency reflectance based on the 30-K microwave data.[4] Other reasonable reflectance extrapolations can shift the frequency of the pinned mode by a factor of 3; in all cases, the conductivity below 3 cm^{-1} is in qualitative agreement with a low-temperature extrapolation of the microwave measurements. Exact agreement is not expected since the pinning frequency varies with impurity concentration and is consequently sample dependent. Dielectric relaxation occurs at frequencies below those shown in the figure. Figure 3(b) shows a similar plot of $\sigma(\omega)$ for the related CDW conductor $(TaSe_4)_2I$, obtained from the literature.[2,11,12] The intrinsic conductivity modes are identified in the figure, along with the giant FIR mode at approximately 10^{12} Hz.

Comparing Figs. 3(a) and 3(b) shows the dramatic difference between the excitation spectra of these two similar CDW materials. Clearly, no giant FIR mode exists in TaS_3. The reflectance edge is a result of a zero crossing of the real part of the dielectric function, but that zero crossing is primarily a manifestation of the microwave pinned acoustic phason mode rather than any

single mode at infrared frequencies. The largest FIR mode in TaS_3 has a relatively small oscillator strength.

We now discuss the implications of these results for general models of CDW conduction. None of the existing models fully explains the conductivity of all three materials. The small size and low frequency of the 8.9-cm^{-1} mode in TaS_3 place constraints on any theory that describes it as a generic mode of similar origin to the large FIR mode seen in $(TaSe_4)_2I$ and $K_{0.3}MoO_3$. To describe the giant FIR mode, Sherwin *et al.*[2] considered an "optical phason" argument similar to the "first-harmonic phason" described earlier by Walker.[13] Lyons and Tucker[14] have attributed the giant FIR mode to coherent oscillations of the CDW phase in tiny regions surrounding impurities. Because each of these models assumes only the presence of a CDW and makes no reference to the crystal structure, each predicts a mode should be present in all CDW materials. The optical phason[2] is estimated to have a frequency near 250 cm^{-1} in TaS_3, and the mode described by Lyons and Tucker[14] should appear at about 85 cm^{-1}. In addition to predicting a mode frequency far higher than that observed, neither model explains why the oscillator strength of a mode in TaS_3 should be more than an order of magnitude smaller than in the other two materials. Though these mechanisms may possibly account for the small high-frequency features in $\epsilon(\omega)$, they do not accurately describe the conductivity of TaS_3 and are thus unlikely explanations for the giant mode seen in other CDW materials.

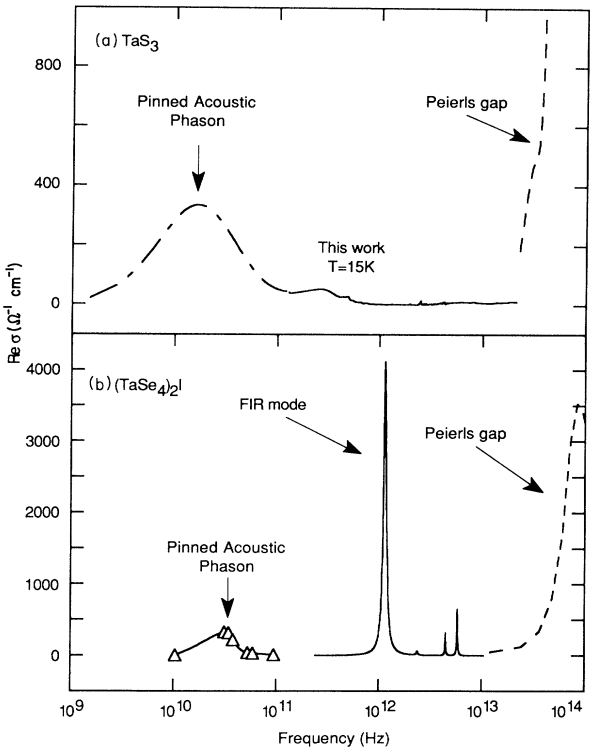

FIG. 3. (a) Reσ for TaS_3. This work is the solid line (intermittently dashed below the measurement limit of 3 cm^{-1}). The dashed line schematically represents the Peierls gap from Ref. 6. (b) Reσ for $(TaSe_4)_2I$ from the literature. The triangles (connected by a line to guide the eye) represent microwave measurements at 50 K from Ref. 11, the solid line is calculated from the FIR oscillators reported in Ref. 2, and the dashed line represents the conductivity near the Peierls gap measured at 140 K in Ref. 12.

A different type of model suggests that the giant FIR mode seen in $(TaSe_4)_2I$ and $K_{0.3}MoO_3$ should be entirely absent in TaS_3.[15,16] This "zone-folding mode generation" model is consistent with our results if the small 8.9-cm^{-1} mode in TaS_3 is entirely unrelated to the giant FIR mode in the other materials. Mode generation through zone folding produces the rich phonon spectrum observed by Raman spectroscopy in semiconductor superlattices[17] and the spin-wave spectrum expected for magnetic superlattices;[18] it was originally considered by Sugai, Sato, and Kurihara in their studies[15,16] of the Raman modes in $(TaSe_4)_2I$. In contrast to the magnetic and semiconductor superlattice systems, which have relatively featureless dispersion curves before the zone folding, CDW materials have a soft Kohn anomaly at $q=2k_F$. In $(TaSe_4)_2I$, a structural distortion expands the unit cell and shrinks the Brillouin zone so that the soft Kohn anomaly phonon is located near the edge of the second Brillouin zone. When the phonon dispersion curve is folded in the reduced-zone scheme, the soft mode lies on a transverse-optical branch above the transverse-acoustic branch. As the temperature is decreased toward T_p, the TO Kohn anomaly begins to soften and triggers the CDW distortion in the usual way, but the interaction between the TO branch and the lower-energy TA branch forces the TA branch to $\omega=0$ first. (Additionally, the degenerate modes at $q=\pm 2k_F$ are mixed to yield both a Raman and an infrared-active mode for each branch.) In this material the observed modes are understood as follows: the pinned acoustic phason mode seen at microwave frequencies arises from the TA anomoly, the giant FIR mode from the TO Kohn anomaly, and the two small higher-frequency modes from two more TO branches also produced by the folding of the original dispersion curve.

A situation analogous to that just described for $(TeSe_4)_2I$ could occur in any CDW material with $2k_F > \pi/a$ (such as $K_{0.3}MoO_3$) with an infrared mode arising through the interaction of the Kohn anomaly phonon with other phonon branches folded into a common region of the Brillouin zone. No such mode should be present in TaS_3 (or $NbSe_3$), where the chains are uniform and the Kohn anomaly is always on the lowest-lying phonon branch.

Though zone-folding mode generation predicts the qualitative difference in $\sigma(\omega)$ between TaS_3 and $(TaSe_4)_2I$ shown in Fig. 3, the plausability of the model awaits a mapping by neutron scattering of the phonon dispersion curve in $(TaSe_4)_2I$. In addition, the model requires a separate explanation for the 8.9-cm^{-1} mode in TaS_3. Initial microwave measurements[4] indicate that below 60 K the CDW is in a glassy state and the conductivity is best described by a broad distribution of pinning energies rather than a single pinning frequency. Within this picture, our measurements suggest that in TaS_3 at low tem-

peratures this distribution is bimodal, with prominent contributions at 0.5 and 8.9 cm^{-1}. The 8.9-cm^{-1} mode weakens rapidly as the temperature is raised from 15 K and appears to be absent by 100 K.

In summary, we have measured the reflectance of TaS_3 and find the FIR conductivity modes to be much smaller than those in two previously measured CDW materials. Though a zone-folding mode generation model may be consistent with this qualitative difference between the various materials, all current models that predict a universal FIR mode in CDW conductors are inconsistent with these results.

We thank B. Burk, D. Miller, and M. Sherwin for useful interactions. This work was supported in part by NSF Grants Nos. DMR 84-00041 and DMR 90-17254, and by the Director, Office of Energy Research, Office of Basic Energy Science, Materials Sciences Division of the U.S. Department of Energy under Contract No. DE-AC03-76SF00098. W.N.C. acknowledges additional support from IBM.

[1]*Charge Density Waves in Solids,* edited by L. P. Gor'kov and G. Grüner (North-Holland, Amsterdam, 1989).
[2]M. S. Sherwin *et al.*, Phys. Rev. B **36**, 6708 (1987).
[3]S. Donovan *et al.* (unpublished).
[4]S. Sridhar *et al.*, Phys. Rev. B **34**, 2223 (1986).
[5]Wei-yu Wu *et al.*, Phys. Rev. Lett. **52**, 2382 (1984); S. Sridhar *et al., ibid.* **55**, 1196 (1985).
[6]S. L. Herr *et al.*, Phys. Rev. B **33**, 8851 (1986).
[7]G. Minton and J. W. Brill, Solid State Commun. **65**, 1069 (1988).
[8]Castin' craft clear casting resin, ETI, Fields Landing, CA 95537.
[9]A. E. Lange *et al.*, Int. J. IR MM Waves **4**, 689 (1983).
[10]These oscillations are due to reflection from the slightly elevated rim of the sample holder. The oscillations die away at higher frequencies as the sample holder becomes effectively a better absorber. Such an artifact cannot be fully removed by the normalization procedure. A line drawn smoothly through the middle of the oscillations should give the true reflectance, and such a line agrees well with the reflectance derived from the microwave conductivity. We used such smoothing in generating the dielectric constant discussed below. Kramers-Kronig transforms performed with and without such smoothing indicate that smoothing the oscillations has no effect on the dielectric constant calculated above 12 cm^{-1}.
[11]Tae Wan Kim *et al.*, Phys. Rev. B **40**, 5372 (1989).
[12]H. P. Geserich, G. Scheiber, M. Dürrler, F. Lévy, and P. Monceau, Physica **143B**, 198 (1986).
[13]M. B. Walker, Can. J. Phys. **56**, 127 (1978).
[14]W. G. Lyons and J. R. Tucker, Phys. Rev. B **40**, 1720 (1989).
[15]S. Sugai *et al.*, Phys. Rev. B **32**, 6809 (1985).
[16]Shunji Sugai *et al.*, Physica **143B**, 195 (1986).
[17]C. Colvard *et al.*, Phys. Rev. Lett. **45**, 298 (1980).
[18]E. L. Albuqueraue *et al.*, Solid State Commun. **58**, 41 (1986).